Mesoporous Aluminosilicates with Ordered Hexagonal Structure, Strong Acidity, and Extraordinary Hydrothermal Stability at High Temperatures

Zongtao Zhang,[†] Yu Han,[†] Feng-Shou Xiao,*[,†] Shilun Qiu,*[,†] Lei Zhu,[†] Runwei Wang,[†] Yi Yu,[†] Ze Zhang,[‡] Bensan Zou,[‡] Yiqian Wang,[‡] Haiping Sun,[‡] Dongyuan Zhao,[§] and Yen Wei[⊥]

Contribution from the Department of Chemistry, Jilin University, Changchun 130023, China, Beijing Lab for Electron Micrography of Center for Condensed Matter Physics & Institute of Physics, Chinese Academic of Sciences, Beijing 10080, China, Department of Chemistry, Fudan University, Shanghai 200433, China, and Department of Chemistry, Drexel University, Philadelphia, Pennsylvania 19104

Received December 1, 2000

Abstract: Highly ordered hexagonal mesoporous aluminosilicates (MAS-5) with uniform pore sizes have been successfully synthesized from assembly of preformed aluminosilcate precursors with cetyltrimethylammonium bromide (CTAB) surfactant. The aluminosilicate precursors were obtained by heating, at 100−140 °C for 2−10 h, aluminasilica gels at the $Al_2O_3/SiO_2/TEAOH/H_2O$ molar ratios of 1.0/7.0−350/10.0−33.0/500−2000. Mesoporous MAS-5 shows extraordinary stability both in boiling water (over 300 h) and in steam (800 °C for 2 h). Temperature-programmed desorption of ammonia shows that the acidic strength of MAS-5 is much higher than that of MCM-41 and is comparable to that of microporous Beta zeolite. In catalytic cracking of 1,3,5-triisopropylbenzene and alkylation of isobutane with butene, MAS-5 exhibits greater catalytic activity and selectivity, as compared with MCM-41 and HZSM-5. The MAS-5 samples were characterized with infrared, UV−Raman, and NMR spectroscopy and numerous other techniques. The results suggest that MAS-5 consists of both mesopores and micropores and that the pore walls of MAS-5 contain primary and secondary structural building units, similar to those of microporous zeolites. Such unique structural features might be responsible for the observed strong acidity and high thermal stability of the mesoporous aluminosilicates with well-ordered hexagonal symmetry.

Introduction

Mesoporous molecular sieves such as hexagonally ordered MCM-41 have attracted much attention because of their potential use as versatile catalysts and catalyst supports for conversion of large molecules.[1−16] However, as compared with conventional zeolites, these mesostructured materials have relatively low acidity and hydrothermal stability, which severely hinders their practical applications in catalytic reactions for the petroleum industry.[1] The relatively low acidity of mesoporous materials such as MCM-41, as compared to zeolites, can be attributed to the amorphous nature of the pore walls.[1,2] To increase the acidity of mesoporous materials, heteropolyacids (HPAs), SO_4^{2-}/ZrO_2, and sulfonic acid groups were supported into the mesopores.[17−19] The HPAs-incorporation approach has successfully generated materials that exhibit good catalytic performance in paraffin isomerization and isobutane/butene alkylation.[17] The sulfonic acid groups have been successfully incorporated into ordered SBA-15 mesoporous silica.[19] However, the success is limited because some pores are blocked by HPAs and SO_4^{2-}/ZrO_2 and the surface area of the materials is reduced significantly.[1,17,18] Therefore, mesoporous materials with strong acidity and uniform pore size as well as large surface area are still being sought.

There have been a number of successful examples for the preparation of mesoporous materials that have reasonably good hydrothermal stability.[1,2−8,14,15] As examples, mesoporous SBA-15 with thick pore walls has been prepared by using triblock

* Address correspondence to these authors: Feng-Shou Xiao (Fax: +86-431-5671974; E-mail: fsxiao@mail.jlu.edu.cn) and Shilun Qiu (E-mail: sqiu@mail.jlu.edu.cn).
[†] Jilin University.
[‡] Chinese Academic of Sciences.
[§] Fudan University.
[⊥] Drexel University.

(1) Corma, A. *Chem. Rev.* **1997**, *97*, 2373.
(2) Kresge, C. T.; Leonowicz, M. E.; Roth, W. J.; Vartuli, J. C.; Beck, J. S. *Nature* **1992**, *352*, 710−712. Beck, J. S.; et al. *J. Am. Chem. Soc*, **1992**, *114*, 10834.
(3) Zhao, D.; Feng, J.; Huo, Q.; Melosh, N.; Fredrickson, G. H.; Chmelka, B. F.; Stucky, G. D. *Science* **1998**, *279*, 548.
(4) Kim, S. S.; Zhang, W.; Pinnavaia, T. J. *Science* **1998**, *282*, 1032.
(5) Ryoo, R.; Kim, J. M.; Shin, C. H. *J. Phys. Chem.* **1996**, *100*, 17718.
(6) Ryoo, R.; Jun, S.; Kin, J. M.; Jim, M. J. *Chem. Commun.* **1997**, 2225.
(7) Mokaya, R.; Jones, W. *Chem. Commun.* **1997**, 2185. Mokaya, R.; Jones, W. *Chem. Commun.* **1998**, 1839.
(8) Mokaya, R. *Angew. Chem., Int. Ed.* **1999**, *38*, 2930.
(9) Huo, Q. S.; et al. *Nature* **1994**, *368*, 317.
(10) Yang, P. D.; Zhao, D. Y.; Margolese, D. I.; Chmelka, B. F.; Stucky, G. D. *Nature* **1998**, *396*, 152.
(11) Antonelli, D. M.; Ying, J. Y. *Curr. Opin. Colloid Interface Sci*. **1996**, *1*, 523−529. Sun, T.; Ying, J. Y. *Nature* **1997**, *389*, 704.
(12) Chen, C.; Li, H.; Davis, M. E. *Microporous Mater*. **1993**, *2*, 17−26.
(13) Khushalani, D.; Kuperman, A.; Coombs, N.; Ozin, G. A. *Chem. Mater*. **1996**, *8*, 2188.
(14) Zhao, X. S.; Lu, G. Q. *J. Phys. Chem. B* **1998**, *102*, 1556.
(15) Kim, J. M.; Jun, S.; Ryoo, R. *J. Phys. Chem. B* **1999**, *103*, 6200.
(16) Yang, P.; Zhao, D.; Margolese, D. J.; Chmelka, B. F.; Stucky, G. D. *Nature* **1998**, *396*, 152−155.
(17) Kozheunikov, I. V.; Sinnema, A.; Jansen, R. J.; Pamin, K.; van Bekkum, H. *Catal. Lett.* **1995**, *30*, 241.
(18) Xia, Q.-H.; Hidajat, K.; Kawi, S. *Chem. Commun.* **2000**, 2229.
(19) Margolese, D.; Melero, J. A.; Christiansen, S. C.; Chmelka, B. F.; Stucky, D. F. *Chem. Mater.* **2000**, *12*, 2448.

10.1021/ja004138t CCC: $20.00
Published on Web 05/04/2001

copolymers as templates.[2] The synthesis of MSU materials has been achieved by using neutral gemini surfactants as the templates.[4] The preparation of KIT-1 involves the use of inorganic salts as additives.[15] Through the grafting route, some stable mesoporous aluminosilicates have been obtained.[5−7] Most of these materials exhibit high hydrothermal stability in boiling water, but few retain the stability under high-temperature steam conditions (e.g., at 800 °C). The latter is much more important because industrial catalysts are usually used under such high-temperature steam conditions.

Despite much encouraging progress in recent years, both the acidity and hydrothermal stability at high temperature of the current mesoporous materials are yet generally lower than those of microporous aluminosilicate zeolites. These drawbacks are probably the main factors that contribute to the lack of large-scale commercial applications of these scientifically interesting materials at the present time. On the other hand, microporous zeolites are very stable, can be made to have high acidity, and, hence, are widely used commercial catalysts, although their applications are intrinsically limited by their small channel diameters. Recently, there were several interesting reports on the synthesis of zeolites with primary and secondary structural building units with structure-directing agents such as aluminosilicate nanoclusters.[20−22] More recently, Firouzi et al. have successfully used cage-like oligomeric silicate species in solution to self-assemble mesoporous materials.[23] Liu et al. have successfully prepared steam-stable aluminosilicate mesostructures assembled from zeolite type Y seeds.[24]

Here we present a unique co-templating approach for the synthesis of new mesoporous aluminosilicates of ordered hexagonal structure with high acidity and excellent hydrothermal stability at high temperatures via self-assembly of aluminosilicate nanoclusters with the templating micella. The materials were thoroughly characterized by means of X-ray diffraction (XRD), transmission electron microscopy (TEM), nitrogen adsorption−desorption isotherm measurements, differential thermal analysis (DTA), and thermogravimetric analysis (TG), as well as infrared (IR), UV−Raman, and ^{27}Al and ^{29}Si nuclear magnetic resonance (NMR) spectroscopy. The acidity of MAS-5 was measured by temperature-programmed desorption of ammonia (NH_3-TPD) and by infrared spectroscopy of adsorbed pyridine on the materials. Catalytic cracking of 1,3,5-triisopropylbenzene and alkylation of isobutane with butene have been investigated by using the new mesoporous aluminosilicates as catalysts. The catalytic activities of new materials are superior over conventional materials such as MCM-41 and HZSM-5, which were studied for direct comparison. Our results show that the new materials contain both mesopores and micropores and that the pore walls consist of both primary and secondary building units, similar to those of microporous zeolites. They might be responsible for the observed high catalytic activity and excellent hydrothermal stability of the new materials. This work, we believe, would open a door for the industrial applications of mesoporous materials as acidic catalysts for large molecular conversions.

Experimental Section

Synthesis. Strongly acidic and hydrothermally stable mesoporous aluminosilicates (denoted as MAS-5) with ordered hexagonal structures were hydrothermally synthesized from starting materials consisting of silica and sodium aluminate (Shenyang Chemical Co., China) in the presence of co-templates, i.e., tetraethylammonium hydroxide (TEAOH, Sinopec, China) and cetyltrimethylammonium bromide (CTAB, Shanghai Chemial Co.) cationic surfactant at Al_2O_3/SiO_2/TEAOH/CTAB/H_2O molar ratios of 1.0/7.0−350/10.0−33.0/12.0−32.0/500−2000. The molar ratio of SiO_2/Al_2O_3 in the final products was varied from 6.0 to 350.

General procedures for preparing MAS-5: (1) First 0.236−1.360 g of sodium aluminate, 0.110−0.400 g of sodium hydroxide, and 26.000−36.000 g of tetraethylammonium hydroxide (20 wt % aqueous solution) were mixed in a plastic vessel. Then 10.086 g of fume silica was added and the reaction mixture was stirred for several hours until a homogeneous solution was obtained. The solution was transferred to Teflon-lined stainless steel autoclaves and heated to 100−150 °C for 2−5 h, yielding aluminosilicate precursors. (2) A mixture of 1.180−1.920 g of CTAB and 25.000 g of deionized water was added into 9.8 g of the aluminosilicate precursors. The resulting mixture was transferred to Teflon-lined stainless-stell autoclaves, again heating at 100−150 °C in an oven. (3) After crystallization for 48 h, the solid product was filtered, washed with water, and dried at 80 °C in air for 12 h. (4) Calcination of the sample was carried out at 550 °C for 6 h in oxygen flow to remove the templates of TEAOH and CTAB. (5) The proton form of the sample was prepared from ion-exchange of NH_4Cl, followed by calcination at 500 °C for 2 h.

MCM-41, HZSM-5, and HBeta are synthesized according to published procedures.[2,22,25]

Characterization. X-ray diffraction (XRD) patterns were obtained with a Siemens D5005 diffractometer using Cu Kα radiation. Transmission electron microscopy (TEM) images and electron diffraction (ED) patterns were recorded on a Philips CM200FEG or a JEM-4000EX electron microscope with an acceleration voltage of 200 kV. The nitrogen isotherms at −196 °C were measured by using a Micromeritics ASAP 2010 system. The samples were outgassed for 2 h at 400 °C before the measurements. The pore-size distribution for mesopores was calculated by using the Barrett−Joyner−Halenda (BJH) model. Adsorption of probing molecules such as 1,3,5-triisopropylbenzene and *n*-hexane was carried out with the Cahn-2000 microbalance at 25 °C. The sensitivity of the microbalance was $\pm$0.1 μg. ^{27}Al NMR spectra were recorded on a Bruker MSL-300WB spectrometer, and chemical shifts were referenced to $Al(H_2O)_6^{3+}$. The Si/Al ratio of the samples was measured by Perkin-Elmer 3300 DV ICP, NMR, and chemical analysis, respectively.

Infrared (IR) spectra of the samples as well as the spectra of pyridine adsorbed on the samples were recorded on a Perkin-Elmer FT-IR spectrometer (PE 430) with a resolution of 1 cm^{-1}. Before measurement of pyridine adsorption, the samples were pressed to thin wafers (5 mg/cm^2) and placed into a quartz cell equipped with CaF_2 windows. The sample disks were evacuated at 400 °C for 2 h (10^{-5} Torr) and cooled to room temperature. Then 10 Torr of pyridine was exposed to the disks at room temperature. After the adsorption at room temperature for 1 h and evacuation at 150 °C for 1 h, the infrared spectra were recorded.

UV−Raman spectra were recorded on a UV−Raman spectrometer built by the State Key Laboratory for Catalysis, Dalian Institute of Chemical Physics, Dalian, China. The UV line excited at 244 nm was from a Coherent Ionva 300 Fred ultraviolet laser instrument equipped with an intracavity frequency-doubling system based on a β-barium borate (BBO) crystal. The laser power at the sample was kept below 4.0 mw. A 180° collection geometry was used to collect the scattered Raman light. The spectral resolution was estimated to be 1.0 cm^{-1}. Powders of samples were pressed into pellets with a diameter of 1.0 cm and placed in a sample holder.

The adsorption of ammonia on the sample was carried out at room temperature, followed by the physical adsorption of ammonia at 120

(20) de Moor, P. E. A.; Beelen, T. P. M.; van Santen, R. A.; Tsuji, T.; Davis, M. E. *Chem. Mater*. **1999**, *11*, 36. de Moor, P. E. A.; Beelen, T. P. M.; van Santen, R. A. *J. Phys. Chem. B* **1999**, *103*, 1639.

(21) Robson, H. *ACS Symp. Ser*. **1989**, *398*, 436.

(22) Zhou, Q.; Pang, W.; Qiu, S.; Jia, M. CN Patent, ZL 93 1 17593.3, 1996. Zhou, Q.; Li, B.; Qiu, S.; Pang, W. *Chem. J. Chin. Univ*. **1999**, *20*, 693−695.

(23) Firouzi, A.; Atef, F.; Oertli, A. G.; Stucky, G. D.; Chmelka, D. F. J. *Am. Chem. Soc*. **1997**, *119*, 3596.

(24) Liu, Y.; Zhang, W.; Pinnavaia, T. J. *J. Am. Chem. Soc*. **2000**, *122*, 8791−8792.

(25) Song, T.; Liu, L.; Xu, R. *Cuihua Xuebao (J. Catal. Chin.)* **1991**, *12*, 283.

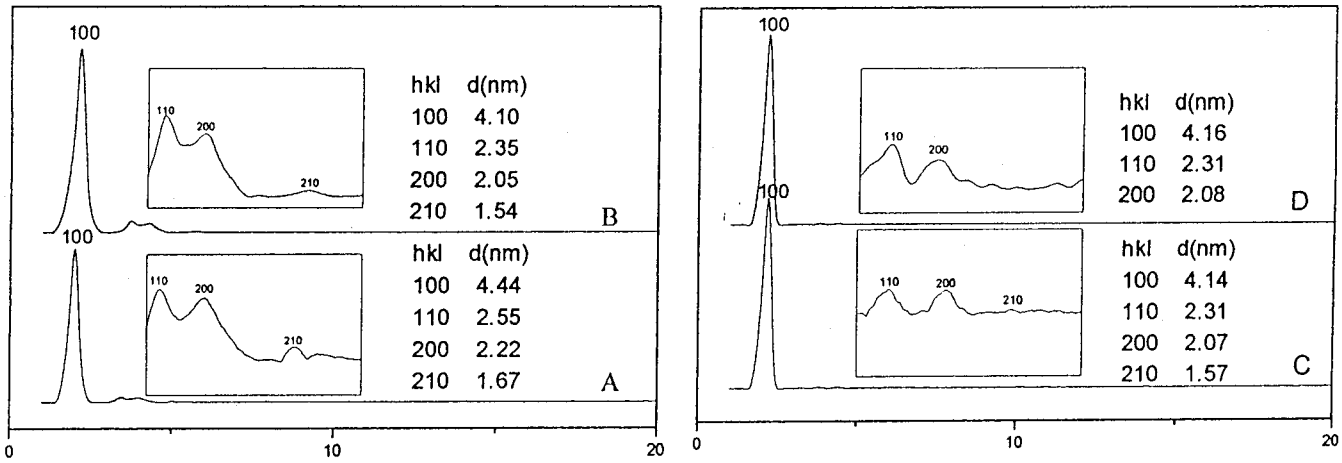

Figure 1. XRD patterns of (A) as-synthesized MAS-5, (B) calcined MAS-5 at 550 °C for 4 h, (C) calcined MAS-5 after treatment in boiling water for 300 h, and (D) calcined MAS-5 after treatment with 100% water steam at 600 °C for 4 h or calcined MAS-5 after treatment with 100% water steam at 800 °C for 2 h.

°C for 1 h in pure nitrogen flow. Temperature-programmed desorption of ammonia (TPD-NH_3) curves was obtained in the range 120−600 °C at a temperature-increasing rate of 15 °C/min. Differential thermal analysis (DTA) and thermogravimetric analysis (TG) were performed on a Perkin-Elmer TGA7 and a DTA-1700, respectively.

Catalytic Reactions. Two catalytic reactions were used to evaluate catalytic performance of the MAS-5 materials, and analyses of the catalytic products were carried out with GC-8A and GC-17A (Shimazu Co.) equipped with TCD and FID detectors. Catalytic cracking of 1,3,5-triisopropylbenzene was carried out by using the pulse method. Samples were calcinated at 600 °C for 5 h to burn off residual organic templates. The catalytic testing was performed according to the following standard conditions: mass of the catalyst was 0.051 g; reaction temperature was in the range 250−320 °C (no thermal cracking); and the ratio of 1,3,5-triisopropylbenzene or isopropylbenzene to the catalyst was 0.4 μL/0.051 g. Nitrogen was used as the carrier gas at a flow rate of 0.92 mL/s.

Catalytic alkylation of isobutane with butene was investigated at a pressure of 2 MPa by using a stainless steel apparatus equipped with a one-through stainless steel flow reactor. Typical reactions were done with 0.5 g of catalyst and at a isobutene/butene (sum of 1-butene and 2-butene) molar ratio of 12/1, 1-butene/2-butene molar ratio of 8/1, and WHSV of 9 h^{-1} at reaction temperatures of 25−100 °C.

Results

X-ray Diffraction. The small-angle X-ray diffraction pattern for a typical as-synthesized MAS-5 sample shows four well-resolved peaks (Figure 1A) that can be indexed as (100), (110), (200), and (210) reflections associated with the hexagonal symmetry. The (100) peak reflects a d spacing of 44.41 Å ($a_0 = 51.33$ Å). No diffraction peak was observed in the region of higher angles 10−40° (Figure 2), which indicates the absence of large microporous crystals in the sample, suggesting that the MAS-5 sample is a pure phase.

After calcination in air at 550 °C for 4 h, the sample XRD pattern (Figure 1B) shows that the four diffraction peaks are still present, confirming that hexagonal MAS-5 is thermally stable. A similarly high degree of mesoscopic order is observed for hexagonal MAS-5 even after calcination to 900 °C. Interestingly, after treatment of the calcined sample in boiling water for more than 300 h (Figure 1C) or at 600 °C for 4 h (or at 800 °C for 2 h) in the flowing water steam (Figure 1D), the XRD patterns show those peaks assigned to the hexagonal symmetry, suggesting that the MAS-5 sample has a remarkable hydrothermal stability even at high temperatures.

Thermal Analysis. In the TG curve the sample shows a weight loss of 51% due to the removal of organic templates of

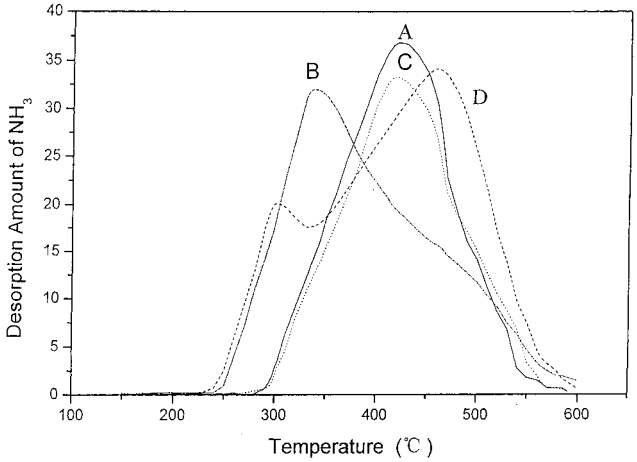

Figure 2. Temperature-programmed desorption of ammonia (NH_3-TPD) curves for various samples of (A) MAS-5, (B) MCM-41, (C) HBeta, and (D) HZSM-5.

TEAOH and CTAB. Simultaneously, in the DTA curve there are obvious peaks at 310−390 and 440 °C, which are reasonably assigned to desorption and decomposition of CTAB and TEAOH, respectively. It is noteworthy that the weight loss of the MAS-5 sample is greater than that of MCM-41 as reported,[1,2] suggesting that MAS-5 has a larger pore volume and more complex porosity.

Acidity. The acidity of the MAS-5 sample was characterized by temperature-programmed desorption of ammonia (NH_3-TPD) and infrared spectroscopy of adsorbed pyridine on the MAS-5 sample. Figure 2 shows NH_3-TPD curves measured on MAS-5, MCM-41, H−ZSM-5, and H-Beta at similar SiO_2/Al_2O_3 ratios (78−84). Apparently, the desorption temperature for ammonia on MAS-5 is about 410 °C, which is much higher than that of MCM-41 (320 °C) at a similar SiO_2/Al_2O_3 ratio. Furthermore, this desorption temperature on MAS-5 is comparable to that of H-Beta zeolite (405 °C).

Types of acidic sites in MAS-5 were investigated by IR spectra of pyridine adsorbed on samples. In general, the band at 1445 cm^{-1} for pyridine adsorbed on the samples is assigned to adsorption of pyridine on Lewis acidic sites, and the band at 1545 cm^{-1} is associated with adsorption of pyridine on Bronsted acidic sites.[26] As shown in Figure 3, both MAS-5 and MCM-41 show the bands at 1445 and 1545 cm^{-1}, but the

(26) Parry, E. P. *J. Catal.* **1963**, *2*, 371.

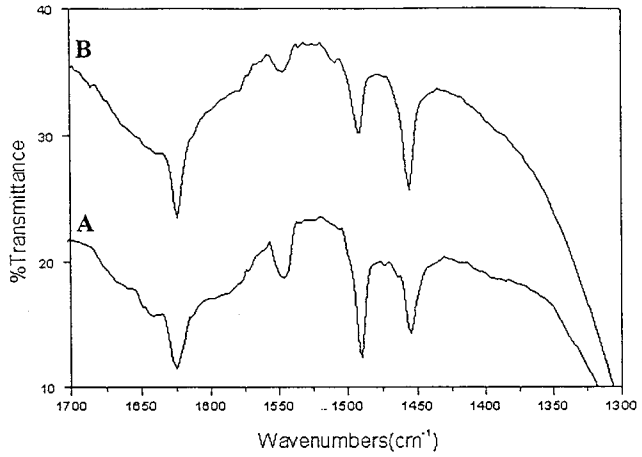

Figure 3. Infrared spectra of pyridine adsorbed on (A) MAS-5 and (B) MCM-41 at room temperature, followed by desorption at 150 °C under vacuum (10^{-5} Torr).

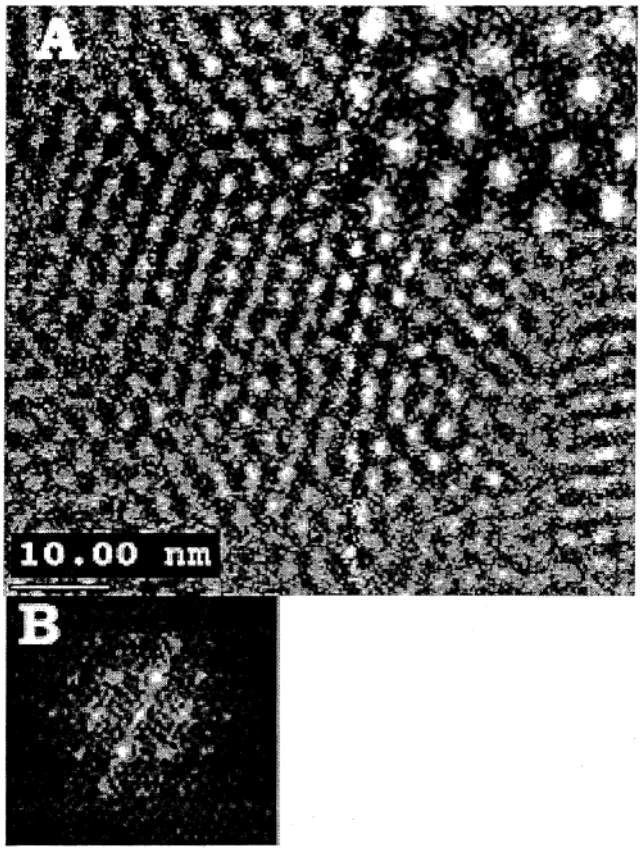

Figure 4. (A) Transmission electron microscopy (TEM) image of calcined MAS-5 (insert: magnification of a region in A for clarity) and (B) beam electron diffraction of calcined MAS-5 for mesopores. The TEM images were obtained on a Philips CM200FEG.

MAS-5 sample gives a much stronger band at 1545 cm^{-1} than MCM-41 does, indicating that MAS-5 has much more Bronsted acidic sites than MCM-41.

Transmission Electron Microscopy. The TEM image of calcined MAS-5 (Figure 4) exhibits ordered hexagonal arrays of mesopores with uniform pore size.[2] The corresponding ED pattern also shows reflections consistent with hexagonal symmetry. From the high-dark contrast in the TEM image of the sample (Figure 4), the distance between mesopores is estimated to be 48 Å, in good agreement with the value determined from XRD.

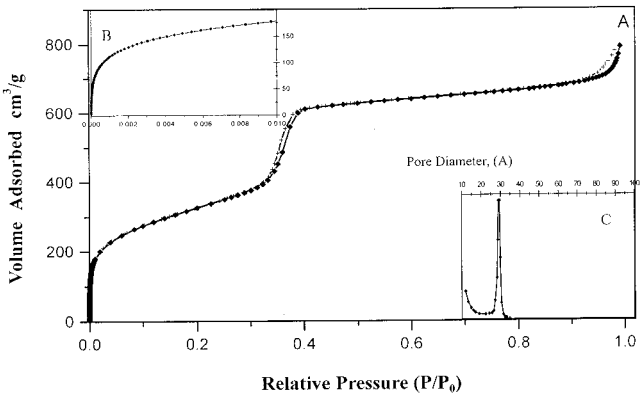

Figure 5. (A) Nitrogen adsorption (+)-desorption (×) isotherm for calcined MAS-5, (B) enlarged adsorption isotherm for calcined MAS-5 in the low-pressure region (10^{-5}—10^{-2} of P/P_0), and (C) mesopore size distribution for calcined MAS-5.

Both pore channels and hexagonal symmetry can be clearly identified in the TEM image for a large area of MAS-5, which indicate that MAS-5 is only one phase. This further confirms that MAS-5 is really a pure phase as indicated by the XRD results. Interestingly, the TEM image viewed down the [110] direction shows that pore channels are not straight, they are arc-like. In contrast, the TEM image recorded along the [110] direction of MCM-41 shows horizontal channels. The arc-like channels may result from the unique preparation of the MAS-5 sample.

Furthermore, as observed in Figure 4 the wall thickness of MAS-5 is greater than that of MCM-41 reported in the literature,[2] which could also be attributed to the unique preparation of MAS-5. The unique preparation is the assembly of CTAB micella with aluminosilicate nanoclusters, and these nanoclusters have stronger rigidity and larger volume in the synthesis of MAS-5 than nonstructure silicon species in the conventional synthesis of MCM-41. The assembly of these nanoclusters needs more space for the clusters to connect to each other.

Adsorption Isotherms. The N_2 adsorption−desorption isotherm of calcined MAS-5 is shown in Figure 5A. It is very interesting to note that the isotherm exhibits a typical adsorption curve of type IV plus type I. A steep increase occurs in the curve at a relative pressure of $10^{-6} < P/P_0 < 0.01$, which is due to the filling of micropores (Figure 5B). Another step can be identified in the adsorption curve at a relative pressure of $0.33 < P/P_0 < 0.40$, which is due to the mesoporous structures. Correspondingly, pore size distribution for calcined MAS-5 shows a narrow uniform pore at the mean value of 27 Å (Figure 5C) assigned to mesopores. Combined with XRD results, we estimate that the thickness of the mesoporous wall is close to 21 Å.

Furthermore, the BET surface area and pore volume of MAS-5 are as high as 1150 m^2/g and 1.17 cm^3/g, respectively. In contrast, we have prepared MCM-41 under the same conditions except for the template of TEAOH, showing the BET surface area and pore volume at 920 m^2/g and 0.68 cm^3/g, which are lower than those of the MAS-5 sample. The parameters of the BET surface area and pore volume of various samples including MAS-5, MCM-41, ZSM-5 zeolite, and a physical mixture of ZSM-5 with MCM-41 are summarized in Table 1. Both MCM-41 and the physical mixtures of ZSM-5 with MCM-41 show lower BET surface area and pore volume than MAS-5. These results indicate that MAS-5 is not a physical mixture of microporous zeolite and mesoporous materials.

Table 1. The Parameters of BET Surface Area and Pore Volume of Various Samples Including MAS-5, MCM-41, ZSM-5 Zeolite, and Physical Mixtures of HZSM-5 Zeolite with MCM-41

sample	BET surface area, m^2/g	pore vol, cm^3/g	micropores Å	mesopores Å
MAS-5[a]	1150	1.17	Yes, 5.8	Yes, 27
MCM-41[b]	940	0.68	No	Yes, 28
ZSM-5	451	0.16	Yes, 5.5	No
MCM-41[c]	980	0.82	No	Yes, 27
physical mixture A[d]	810	0.55	Yes, 5.5	Yes, 28
physical mixture B[e]	732	0.45	Yes, 5.5	Yes, 28

[a] MAS-5 was prepared from self-assembly of CTAB with aluminosilicate nanoclusters with primary and secondary zeolite building units, and the aluminosilicate nanoclusters were formed by heating of $Al_2O_3-SiO_2$ (Si/Al = 30) gels for several hours at 100−140 °C in the presence of TEAOH. [b] MCM-41 was prepared from self-assembly of CTAB with $Al_2O_3-SiO_2$ (Si/Al = 30) gels without addition of TEAOH [ref 2]. [c] MCM-41 was prepared from self-assembly of CTAB, TEAOH, and $Al_2O_3-SiO_2$ (Si/Al = 30) gels, and the addition of CTAB and TEAOH is the beginning of the synthesis; synthesis procedures are similar to those reported by Das et al.[33] [d] 30% ZSM-5 + 70% MCM-41, g/g. [e] 50% ZSM-5 + 50% MCM-41, g/g.

Probing molecules of 1,3,5-triisopropylbenzene and *n*-hexane were also used to characterize the nature of porosity in MAS-5 materials. At first, the calcined MAS-5 sample was evacuated at 400 °C for 4 h to remove molecules adsorbed on the pores, followed by cooling the sample to 25 °C. Then, 1,3,5-triisopropylbenzene was exposed to the MAS-5 sample for 4 h to reach adsorption saturation (saturation amount of 0.67 g/g). Finally, *n*-hexane was introduced into the MAS-5 sample that was already saturated with adsorbed 1,3,5-triisopropylbenzene. It is very interesting indeed that a large amount of *n*-hexane, 0.11 g/g ($P/P_0 = 0.3$), was adsorbed in the MAS-5 sample saturated with 1,3,5-triisopropylbenzene, indicating the presence of micropores in MAS-5 materials. This phenomenon can be readily explained based on the model that MAS-5 has both mesopores and micropores. Thus, 1,3,5-triisopropylbenzene having a large size (~13 Å) can be adsorbed in mesopores, and it cannot be adsorbed in micropores due to the small size of the micropores. After saturation with 1,3,5-triisopropylbenzene in mesopores, the vacant micropores in MAS-5 materials are still available for adsorption of smaller hexane molecules. In sharp contrast, our control experiments show that the MCM-41 samples that were saturated with 1,3,5-triisopropylbenzene adsorbed only a very small amount of *n*-hexane (<0.03 g/g at $P/P_0 = 0.3$) under identical conditions.

IR Spectroscopy. Figure 6 gives the mid-infrared spectra of MCM-41 and MAS-5 at a similar Si/Al ratio. The IR spectrum of MCM-41 shows a borad band at 460 cm^{-1} in the region of 400−600 cm^{-1}, which is similar to those of amorphous materials. However, MAS-5 exhibits four sharp bands at 410−480 cm^{-1} and additional bands at 520−600 cm^{-1} in the region of 400−600 cm^{-1}, which are similar to those of six- or five-membered rings of T−O−T (T = Si or Al) in microporous zeolites.[27] These results suggest that MAS-5 has zeolite primary and secondary building units.

Furthermore, the preparation of aluminosilicate precursors from TEAOH has also been monitored with IR spectroscopy. When sodium aluminate was mixed with silica in the presence of TEAOH solution at room temperature, the IR spectrum does not show the bands at 520−600 cm^{-1} assigned to five-membered rings of T−O−T. After the aluminosilicate gel was heated in the presence of TEAOH at 100−140 °C for several hours, the precursors for preparing MAS-5 were formed, which give rise to a band at 520−600 cm^{-1}, indicating the existence of zeolite primary and secondary building units in these precursors, possibly assignable to aluminosilicate nanoclusters. In contrast, the same treatment for the aluminosilicate gel in the absence of TEAOH did not cause the appearance of this band.

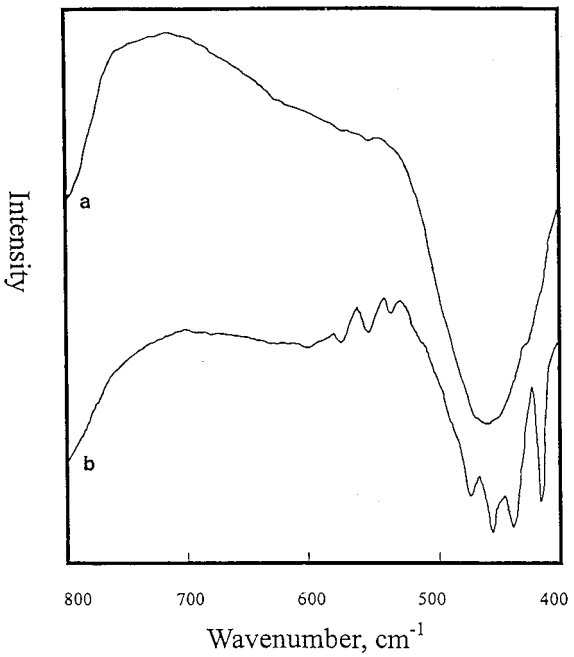

Figure 6. IR spectra of (a) MCM-41 and (b) MAS-5 after removal of organic templates.

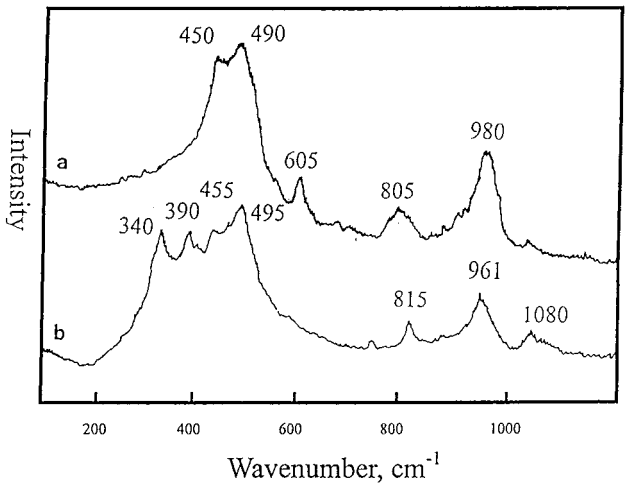

Figure 7. UV Raman spectra of (a) MCM-41 and (b) MAS-5.

UV−Raman Spectrosocpy. UV−Raman spectra of MCM-41 and MAS-5 are shown in Figure 7. The Raman spectrum of MCM-41 shows typical bands at 450 and 490, 605, 805, and 980 cm^{-1}, in good agreement with those in the literature.[28,29] However, the band at 605 cm^{-1} assigned to three-membered rings (T−O−T) in amorphous silica[27] disappeared completely in the MAS-5 sample. On the other hand, crystalline molecular sieves containing three-membered rings such as lovdarite and VPI-7 do not have the Raman band at 604 cm^{-1}.[30]

(27) Breck, D. W., Ed. *Zeolite Molecular Sieves*; Wiely: New York, 1974. Jabobs, P. A.; Derouane, E. G.; Weitkamp, J. *J. Chem. Soc., Chem. Commun.* **1981**, 591.

(28) Chen, C. Y.; Li, H.-X.; Davis, M. E. *Microporous Mater.* **1993**, *2*, 17.

(29) Xiong, G.; Li, C.; Li, H.; Xin, Q.; Feng, Z. *Chem. Commun.* **2000**, 667.

(30) Annen, M. J.; Davis, M. E. *Microporous Mater.* **1993**, *1*, 57.

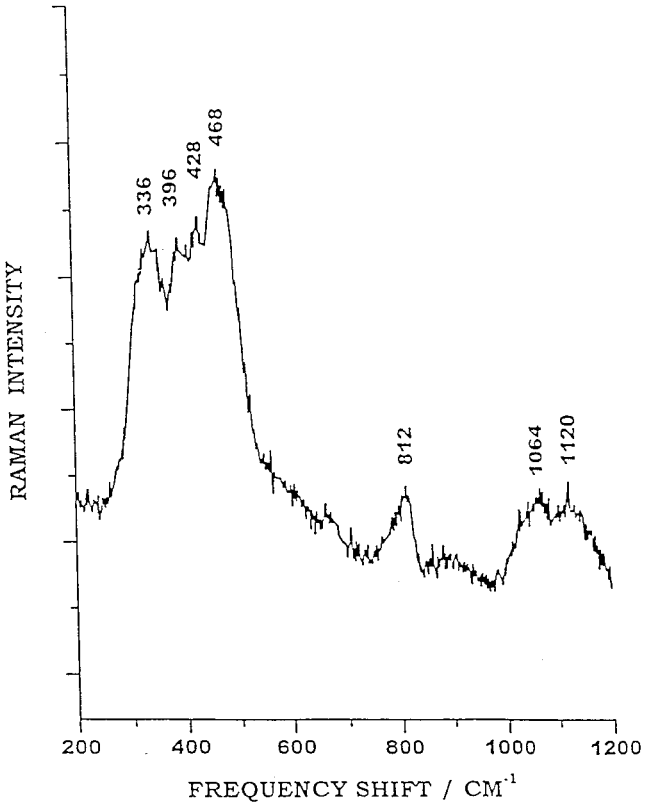

Figure 8. UV Raman spectrum of zeolite Beta.

In our case, the spectrum of MAS-5 exhibits new bands at 340 and 390 cm^{-1} assigned to five-membered rings of T−O−T.[31,32] These results suggest that the wall of the MAS-5 sample is not amorphous, and that there are zeolite primary and secondary structure building units such as the five-membered ring of T−O−T in the MAS-5 sample.

Furthermore, we observed that the UV−Raman band for MAS-5 has a similar frequency to that for Beta zeolite (Figure 8) although the band intensity for MAS-5 is much weaker. Such an observation implies that the zeolite primary and secondary structure building units in MAS-5 might be similar to those in Beta zeolite.

NMR Spectrosocpy. MAS-5, MCM-41, and Beta zeolite were studied by ^{27}Al and ^{29}Si NMR spectroscopy, and Figure 9 shows ^{27}Al NMR spectra for these samples. Obviously, full-width half-height (fwhh) of MAS-5 is close to that of Beta zeolite, much narrower than that of MCM-41, suggesting the order of Al species in the MAS-5 sample is better than that of MCM-41. Furthermore, we observed the peak position of ^{27}Al NMR for MAS-5 appears at 61 ppm, which is also closed to that of zeolite Beta. In contrast, MCM-41 exhibits this peak at 55 ppm.

Catalytic Cracking. Catalytic activities in the cracking of 1,3,5-triisopropylbenzene over various catalysts are summarized in Table 2. HZSM-5 is almost inactive due to its relatively small pore size and large diameter of reactant molecules. MCM-41 shows high activity. However, it completely losses its activity after treatment in boiling water for 6 h or 600 °C for 2 h. In contrast, the calcined MAS-5 gives both higher activity and longer catalyst life than MCM-41. More significantly, after treatment in boiling water for 300 h, at 600 °C for 4 h, or at 800 °C for 2 h, MAS-5 still shows high catalytic activity. These observations further confirm that MAS-5 has a strong acidity and high hydrothermal stability. MAS-5 is an excellent candidate as a catalyst for industrial cracking of petroleum, particularly of the petroleum residues for which high reaction temperatures are required.[1]

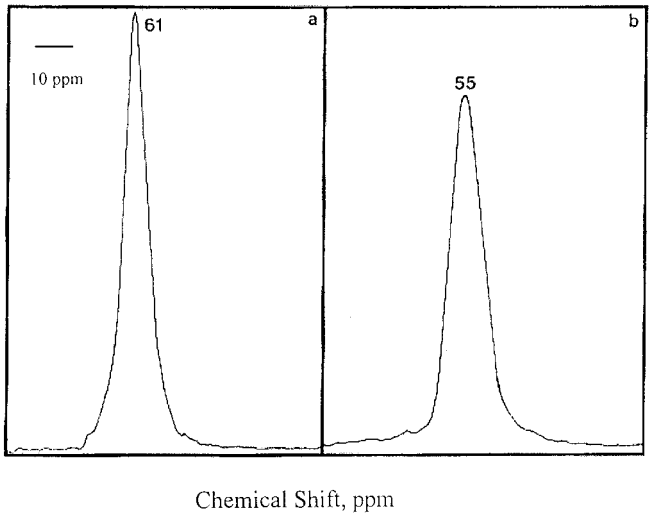

Figure 9. ^{27}Al NMR spectra of (a) MCM-41 and (b) MAS-5.

Table 2. Catalytic Activities in Cracking of 1,3,5-Triisopropylbenzene on Various Catalysts[a]

sample	SiO_2/Al_2O_3	treatment	conversion, %	reaction temp, °C
HZSM-5	84		1.7	250
HMCM-41	80		65.8	250
HMCM-41	80	boiling water for 6 h	<1.0	250
HMCM-41	80	treated with 100% water vapor at 600 °C for 2 h	<1.0	250
MAS-5	81		78.8	250
MAS-5	81	boiling water for 300 h	79.1	250
MAS-5	81	treated with 100% water vapor at 600 °C for 4 h	78.9	250
MAS-5	80	treated with 100% water vapor at 800 °C for 2 h	77.5	250
MAS-5	123		87.0	320
MAS-5	81		90.1	320
MAS-5	59		95.2	320

[a] Catalytic reactions were performed by pulse injections, and the data presented in this table are the average values of 5 injections. In each run, 50 mg of catalyst was used, pulse injection of the reactant was 0.4 μL, and the reaction flow rate was 53.7 mL/min.

Catalytic Alkylation. As shown in Figure 10, MAS-5 exhibits higher activity in the catalytic alkylation of isobutane with butene than the calcined MCM-41 at a similar SiO_2/Al_2O_3 ratio, which is attributed to strong acidic sites in MAS-5. Furthermore, the activity of MAS-5 was found to be higher than that of Beta zeolite. As depicted in Figure 2, both the acidity and number of acidic sites in MAS-5 and Beta are similar, and the difference in the activity between MAS-5 and Beta could not be assigned to the change in acidity. One possibility is that MAS-5 might be advantageous because of its unique structure of coexistence of both micropores and mesopores. Moreover, as demonstrated in Figure 10, MAS-5 shows the lowest coke formation. This could also be attributed to the unique structure of both micropores and mesopores so that mesopores allow for easier diffusion of products as compared with micropores.

Discussion

Hydrothermal Stability and Acidity. The hydrothermal stability of various samples, including MAS-5, MCM-41

(31) Li, C.; Xiong, G.; Xin, Q.; Liu, J.; Ying, P.; Feng, Z.; Li, J.; Yang, W.; Wang, Y.; Wang, G.; Liu, X.; Lin, M.; Wang, X.; Min, E. *Angew. Chem., Int. Ed.* **1999**, *38*, 2220.
(32) Yu, Y.; Xiong, G.; Li, C.; Xiao, F.-S. *J. Catal.* **2000**, *194*, 487.

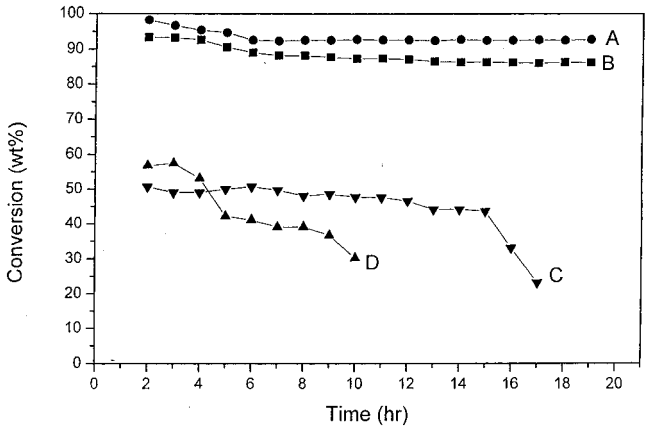

Figure 10. Catalytic conversion of 2-butene in alkylation of isobutane with butene vs reaction time over various catalysts (each of 0.5 g) of (A) MAS-5, (B) HBeta, (C) MCM-41, and (D) HZSM-5 at a reaction temperature of 25 °C with a isobutane/butene molar ratio of 12/1, a 1-butene/2-butene molar ratio of 8/1, and WHSV of 9 h^{-1}.

Table 3. Evaluation of Hydrothermal Stability of Various Samples[a]

sample	stability, h: in boiling water	in steam at 600 °C	in steam at 800 °C	refs
Beta zeolite	>300	>6	>4	
MAS-5	>300	>6	2−3	
MCM-41 from Beck	<12	<4		2
MCM-41 from Das	100	<6	<1	33
MCM-41 from Kawi	120	<6	<1	34
MCM-41 from Mokaya	180		<2	8
ZSM-5/MCM-41 from van Bekkum	120	<6	<1	35
MSU−S from Pinnavaia	<200		>2	35

[a] Various samples were synthesized in our laboratories according to the literature procedures. Upon hydrothermal treatment, the samples were characterized by XRD and BET surface area. All the hydrothermal stability evaluations were made under the same experimental conditions.

prepared from Beck's method,[2] MCM-41 prepared from Das' method,[33] MCM-41 prepared from Kawi's method,[34] ZSM-5/MCM-41 prepared from van Bekkum's method,[35] and MSU-S prepared from Pinnavaia's method,[24] has been evaluated under identical conditions and data are summarized in Table 3. MAS-5 materials are remarkably stable in boiling water for more than 300 h. In comparison, all other mesoporous materials failed under these conditions. It is quite clear that the hydrothermal stability of MAS-5 is the highest among all the mesoporous materials examined and is comparable to that of microporous Beta zeolite.

Besides the superior hydrothermal stability, MAS-5 with a uniform pore size of 27 Å and large surface area of 1170 m^2/g shows very high acidity, similar to that of Beta zeolite, without any postsynthesis modifications such as the incorporation of heteropolyacids in mesopores.[17] This would be of great advantage for industrial applications in catalytic reactions such as petroleum refining.

MAS-5 Phase Purity. As suggested by the results of nitrogen adsorption isotherms (Figure 5) and adsorption of probing molecules, MAS-5 materials possess both micropores and mesopores. There are two main possibilities for the observation of such structures: the materials are merely physical mixtures of independent microporous zeolitic and mesoporous components or they are truly bifunctional with micropores integrated into the mesoporous structure framework. The following evidence strongly argues for MAS-5 as bifunctional pure phase materials.

(1) We have collected over 500 TEM images and carefully examined various domains in the MAS-5 samples. In all of the TEM images, the materials exhibit well-ordered hexagonal mesopores and no the other phases were observed. There is no region that might be identifiable as a mixture of microporous zeolite and mesoporous materials (e.g., Figure 4).

(2) Comparison of surface area and pore volume of various samples demonstrates that the surface area and pore volume of MAS-5 are higher than those of MCM-41, although both were prepared with the same templates, i.e., TEAOH and CTAB (Table 1). If there is a physical mixture of microporous zeolite and mesoporous materials, its specific surface area and pore volume should be lower than those of MCM-41.

(3) The XRD pattern for MAS-5 only shows several peaks in the small-angle region (0.1−6°) associated with a hexagonal symmetry for mesopores. There is no distinguishable peak in the wide-angle region (10−40°), which suggests that there are no large microporous crystals in the MAS-5 sample. That is, the packing of micropores in MAS-5 should be largely disordered. On the other hand, physical mixtures of microporous zeolites and mesoporous materials generally exhibit both XRD peaks for mesoporous materials and for microporous zeolites. It was also reported that mixtures of MFI zeolite and MCM-41 show both peaks of MFI zeolite and those of MCM-41 in the their XRD patterns.[36,37]

(4) In the TPD-NH_3 curves for acidity evaluation, a physical mixture of MCM-41 and Beta zeolite shows two distinct peaks at 310 and 405 °C, respectively, while MAS-5 shows only one peak at 410 °C.

(5) In the UV−Raman spectroscopic study, if the sample were a physical mixture, we should observe the band at 604 cm^{-1} assigned to amorphous silica in the mesopore walls.[30] We did not find this band in the MAS-5 materials.

(6) In the ^{27}Al NMR spectra, if the sample were a physical mixture there should be a signal at 53−56 ppm with similar fwhh to that of MCM-41. The fact is that the chemical shift of ^{27}Al in MAS-5 is 61 ppm, which is different from that in MCM-41.

(7) Catalytic alkylation of isobutane with butene (Figure 10) shows that MAS-5 exhibits higher catalytic activity than that of calcined MCM-41 and Beta zeolite at a similar SiO_2/Al_2O_3 ratio. If MAS-5 were a physical mixture of microporous zeolite like Beta and mesoporous materials such as MCM-41, its catalytic activity should be lower than that of Beta zeolite.

In sum, all the above observations suggest that MAS-5 is not merely a physical mixture of microporous zeolite and mesoporous materials but also pure phase integrated bifunctional molecular sieves. Further investigation is in progress in an effort to achieve unambiguous, preferrably micrographic, identification and characterization of the micropore structure in the MAS-5 materials.

Preparation of MAS-5 by Precursors. The observed superior hydrothermal stability, acidity, catalytic activity, and intriguing bifunctional structures might be associated with our unique approach for the synthesis of the MAS-5 materials. It has been reported that chemical and physical properties of

(33) Das, D.; Tsai, C. M.; Cheng, S. *Chem. Commun.* **1999**, 473−474.
(34) Shen, S.-C.; Kawi, S. *J. Phys. Chem. B* **1999**, *103*, 8870−8876.
(35) Kloetstra, K. R.; van Bekkum, H.; Jansen, R. J. *Chem. Commun.* **1999**, 2281−2282.
(36) Karlsson, A.; Stoker, M.; Schmidt, R. *Microporous Mesoporous Mater.* **1999**, *27*, 181−192.
(37) Huang, L.; Guo, W.; Deng, P.; Xue, Z.; Li, Q. *J. Phys. Chem.* **2000**, *104*, 2817.

MCM-41 are strongly dependent on the preparation conditions.[1−16] In the case of MAS-5, the key point for the synthesis is, we believe, the preformation of aluminosilcate precursors which could undergo assembly with the CTAB micella to generate mesostructures.

The aluminosilicate precursors were prepared by heating aluminosilicate gel in the presence of TEAOH at 100−140 °C for 2−3 h. TEAOH is known to be a very good structure-directing agent in the synthesis of Beta zeolite.[22] We have reported that addition of a small amount of aluminosilicate precursors (3 wt %) into alumina-silica gel ($Al_2O_3/SiO_2/Na_2O/H_2O$ = 1/10−40/2.8−12/500−900) at 140 °C for 2−4 days leads to Beta zeolite with high crystallinity in the absence of organic templates.[22] The aluminosilicate precursors appear to serve as seeds for the formation of Beta zeolite.[22] Recently, a similar idea has been reported by Liu et al., and they used zeolite type Y seeds to self-assemble mesoporous materials.[24] IR characterization of our aluminosilicate precursors shows a clear band at 520−600 cm^{-1}, which is characteristic of five-membered rings, indicating that aluminosilicate precursors contain zeolite primary and secondary structure building units.[27] On the basis of all these observations, we propose a tentative mechanism for the formation of mesoporous MAS-5 materials containing disordered micropores via the self-assembly of aluminosilicate precursors, as nanoclusters with zeolite primary and secondary structure building units, with CTAB micella.

Since the aluminosilicate precursors contain zeolite primary and secondary structure building units, the size of aluminosilicate precursor particles (or nanoclusters) should be larger than that of SiO_4 or AlO_4 tedtrahedrons for constructing the walls of mesopores. As a consequence, the pore walls in MAS-5 should, and were found to, be thicker than that in MCM-41, which is assembled from SiO_4 or AlO_4 tedtrahedrons. Such thicker walls in MAS-5 might contribute significantly to the excellent hydrothermal stability. On the other hand, micropores with Beta zeolite-like properties preserved in the precursor particles might account for the observed high acidity of MAS-5 materials. In addition, the large particle size of aluminosilicate precursors should have some rigidity for assembly with CTAB micella, which might lead to the formation of arc-like pore channels. In most of the literature procedures for the synthesis of mesoporous materials, the mesostructure is generally built from SiO_4 and AlO_4 tetrahedron building blocks, even though both TEAOH and CTAB, as employed in this study, are used as templates.[8,34,35] There is little chance, under those synthetic conditions, for the formation of the aluminosilicate nanoclusters with zeolite primary and secondary structure building units. Therefore, there are many fewer micropores in those mesoporous materials than in MAS-5. Currently we are carrying out further experiments to elucidate the mechanism and to explore the applications of this concept in the synthesis of other material systems.

Conclusions

Mesoporous aluminosilicates (MAS-5) with ordered hexagonal structure have been prepared hydrothermally from preformed aluminosilcate precursors with CTAB surfactant as the template. The materials have a large surface area of 1170 m^2/g and a uniform mesoporous diameter of 27 Å, and exhibit extraordinarily good hydrothermal stability and high acidity, both comparable to microporous Beta zeolite and superior over most other mesoporous materials. Characterization results indicate that MAS-5 materials possess both micropores and mesopores and that the mesopore walls contain the primary and secondary building units similar to those in microporous zeolites. In catalytic cracking of 1,3,5-triisopropylbenzene and alkylation of isobutane with butene, MAS-5 materials show greater catalytic activity and selectivity as well as longer catalyst lifetime in comparison with MCM-41 and HZSM-5 materials.

Acknowledgment. We thank Professor Ruren Xu of Jilin University for helpful suggestions and discussions. We are most grateful to Professor Osamu Tarasaki of Tohoku University, Japan, for his assistance in TEM measurements. This work was supported by the State Basic Research Project of China (Grant No. G2000077507), the National Natural Science Foundation of China (NSFC, Grant Nos. 29825108 and 29733070), and the National Advanced Materials Committee of China (NAMCC, Grant No. 863-715-004-0210).

Supporting Information Available: Figures showing the XRD pattern of MAS-5, DTA and TG curves of MAS-5, a TEM image of calcined MAS-5, IR spectra, and the proposed tentative mechanism of MAS-5 formation (PDF). This material is available free of charge via the Internet at http://pubs.acs.org.

JA004138T